NATIONAL ADVISORY COMMITTEE FOR AERONAUTICS

TECHNICAL NOTE

No. 1746

FLOW OF A COMPRESSIBLE FLUID PAST A SYMMETRICAL AIRFOIL IN A WIND TUNNEL AND IN FREE AIR

By Howard W. Emmons

Harvard University

Washington

November 1948

NATIONAL ADVISORY COMMITTEE FOR AERONAUTICS

TECHNICAL NOTE NO. 1746

FLOW OF A COMPRESSIBLE FLUID PAST A SYMMETRICAL AIRFOIL IN A WIND TUNNEL AND IN FREE AIR

By Howard W. Emmons

SUMMARY

The effects of compressibility on the flow about the NACA 0012 airfoil in a wind tunnel and in free air have been investigated by the relaxation method. The details of how the numerical work is carried out have been described previously. The solutions obtained cover the incompressible case, the cases when the entire flow is subsonic, the case when supersonic regions are present, and several cases when the supersonic region terminates in shock waves, that is, post-critical flow. Comparisons are made with experimental results and with approximate theories for the compressibility effects and for wind-tunnel interference.

The calculated results describe compressibility effects, as observed experimentally, considerably better than any of the well-known compressibility correction formulas. The predicted post-critical flow patterns, including the shock waves if present, agree well with experimental pressure distributions. The results calculated by this method agree with experimental results as well as possible for any theory based upon a frictionless-fluid model. To include friction in the calculations involves considerably greater computation time and a modern sequence-controlled calculator is indicated.

INTRODUCTION

The effect of compressibility on airfoil performance is for most practical purposes negligible for velocities less than about 0.3 of the speed of sound. Above this Mach number the effects of compressibility increase more and more rapidly until they assume major importance in the aerodynamic performance of airfoils and other bodies. A number of more or less successful attempts have been made to predict in an approximate way the effects of compressibility. Perhaps the best-known formulas for the correction of the flow about a body are those of Prandtl, Glauert, Von Kármán, and Tsien (references 1 to 4, respectively). In all these compressibility correction formulas, high accuracy is attained for small deviations from the incompressible flow, but the accuracy decreases as

the Mach number increases. In no case has it been possible to predict the precise Mach number at which shock waves first appear nor to give any picture at all of the flow about the body after shock waves are present. In fact, there are no analytical methods available at the present time which appear to be adequate to obtain solutions of the flow about a body when shock waves are present. Besides the serious effects of compressibility on airplane performance and on ability to predict theoretically what will happen, there is an additional serious difficulty which arises in attempting to study these effects experimentally. The best method of studying aerodynamic performance that has been developed is the use of wind tunnels. The wind-tunnel walls introduce effects which are not present for the same body flying in free air, and wind-tunnel results must, therefore, be corrected for the effects of the walls if accurate predictions are to be made for flight in free air. Theoretical predictions of the effect of wind-tunnel walls for incompressible fluids have been successful with the required accuracy. For increasing Mach numbers, however, the corrections increase very rapidly and have a very profound effect on the flow as shock waves appear. Thus, the best experimental method in aerodynamics is seriously handicapped by the lack of knowledge of what wind-tunnel-wall corrections should be made to wind-tunnel test results.

In several reports (references 5 to 8) the relaxation method for the numerical solution of partial differential equations has been extended to include the flow of compressible fluids. In the present report these methods are used to compute the flow about an airfoil in a wind tunnel and in free air. Several years ago when this work was started, tests were planned by the NACA for the symmetrical NACA 0012 airfoil with a 5-inch chord in an 18-inch two-dimensional wind tunnel. These tests were to involve among other things pressure-distribution measurements at zero angle of attack of the airfoil so that this particular arrangement was decided upon for the present computations.

This work was done at Harvard University under the sponsorship and with the financial assistance of the National Advisory Committee for Aeronautics.

The author acknowledges the very able and patient efforts of Dr. Priscilla F. Bok, who carried out the involved numerical computations required to obtain the solutions presented in this report.

SYMBOLS

c airfoil chord

C_{p_M} pressure coefficient $\left(\frac{p - p_1}{\frac{1}{2}\rho_1 q_1^2}\right)$.

C_{p_0}	pressure coefficient for incompressible fluid, i.e., M = 0
H	tunnel height
M	local Mach number
M_1	Mach number of undisturbed stream
p	local static pressure
p_1	static pressure of undisturbed stream
p_0	stagnation pressure of undisturbed stream
q	local velocity
q_1	velocity of undisturbed stream
q_i	velocity relative to velocity of undisturbed stream (q/q_1)
t	airfoil thickness
α	angle of attack
γ	isentropic exponent
ψ	stream function for compressible fluid
η	stream function for incompressible fluids
ρ	mass density of fluid
ρ_1	mass density of fluid in undisturbed stream
ξ	velocity potential for incompressible fluid

PROCEDURE

The calculations have been carried out essentially as described in reference 5. The first step was to compute and draw the airfoil accurately on the center line of the wind tunnel with the dimensions mentioned previously. (See fig. 1.) By numerical calculations, the incompressible stream function η and velocity potential ξ were computed and were then used as a coordinate system for the calculation

of the flow of the compressible fluid. The actual calculations were carried out by a square network of points which were widely spaced (2 in.) far from the airfoil and were very closely spaced at the critical sections of the airfoil surface itself. The smallest nets used were 1/32 inch (as compared with the 5-in. chord). These fine nets were used at the nose of the airfoil where conditions change very rapidly near the stagnation point and also on the surface of the airfoil near the nose where the velocity is highest and hence where the greatest accuracy is required for the compressibility corrections. A total of about 600 points was used. If the finest net had been extended through the entire region, about 200,000 points would have been needed. The stream function η was first computed. The Cauchy-Riemann equations in finite-difference form were then used to compute the velocity potential ξ. The accuracy of the velocity potential thus obtained was not so high as for η but was increased to this accuracy by relaxation.

In figure 1 the geometry and essential dimensions of the airfoil in the tunnel are shown, and in figure 2 the streamlines, equipotential lines, and constant-velocity lines are drawn for the incompressible flow. The values on the constant velocity lines are indicated by values of q_i which are equal to the velocity of the fluid at that point divided by the velocity of the fluid at infinity. The accuracy of the numerical calculation is considerably higher than can be shown in figure 2. The calculations were made with five digits. The stream function on the center line of the tunnel and on the surface of the airfoil was taken as zero while that on the tunnel wall was taken as 90,000. This large number of decimal places is required if reasonable accuracy in the value of q_i is to be obtained, and accurate q_i values are essential for the relatively sensitive effects at high Mach numbers. The precise accuracy for the value of q_i is difficult to estimate.

RESULTS AND DISCUSSION

The calculations for the airfoil in free air gave results which look essentially like figure 2. The differences are very small and the significant differences are better indicated in terms of the pressure coefficient and the so-called induced velocity.

In figure 3 the distribution of pressure coefficient along the chord of the airfoil is shown for the airfoil in the tunnel and the airfoil in free air. The pressure coefficient is defined by

$$C_{p_0} = \frac{p - p_1}{\frac{1}{2}\rho_1 q_1^2}$$

$$= 1 - \left(\frac{q}{q_1}\right)^2$$

$$= 1 - q_1^2 \qquad (1)$$

Note from this equation that the deviation of q_1^2 from 1 gives the pressure coefficient and hence one decimal place of accuracy is lost immediately upon computing a pressure coefficient. It is for this reason that a large number of decimal places is required for the original calculation. Note in figure 3 that the difference between the coefficients in the wind tunnel and in free air is only about 4 percent of the maximum coefficient. In figure 3 there are plotted for comparison the calculations made at the NACA, using Theodorsen's method (references 9 and 10). No attempt has been made to reexamine his method to see whether the deviations found are to be expected. It is not possible to locate the cause of this difference without a considerable reexamination of both calculations. The pressure coefficient for the airfoil in the tunnel is everywhere of slightly greater magnitude than that for the airfoil in free air. This is physically to be expected since, with a wind-tunnel wall present, there is more "venturi" effect than if no restraint had been placed on the shape of the streamlines distant from the airfoil.

The effect of the wind-tunnel wall can also be considered as represented by the change in velocity at any point in the air stream produced by the introduction of the tunnel walls. In figure 4 the velocity induced by wind-tunnel walls in the narrowest section between the airfoil and the tunnel is shown as computed from approximate analytical expressions presented by Thom (reference 11) and as computed by the relaxation method.

After computing the foregoing incompressible solutions, the flow of a compressible fluid was computed for a series of Mach numbers by using the stream function and velocity potential as a coordinate system. This avoids the use of awkward boundary conditions since now the entire boundary consisting of the symmetrical axis of the tunnel plus the surface of the airfoil becomes a single straight line. The following table shows the cases calculated for Mach numbers of the undisturbed stream.

Airfoil in tunnel	Airfoil in free air
$M_1 = 0$	$M_1 = 0$
$M_1 = 0.4$	$M_1 = 0.7$
$M_1 = 0.6$	$M_1 = 0.75$; no shock wave present
$M_1 = 0.7$	
$M_1 = 0.73$; no shock wave present	
$M_1 = 0.74$; shock wave present	
$M_1 = 0.75$; shock wave present	

The calculations for the compressible fluid under those subsonic conditions for which no supersonic region appears are very simple to carry through. As a supersonic region appears, and particularly as shock waves are required, the solution becomes increasingly difficult to obtain, and it is often impossible to get any particular solution on the first attempt. For the airfoil in the tunnel, for example, computations were made in the order $M_1 = 0$, 0.4, 0.6, and 0.7. On carrying out the solution at $M_1 = 0.7$, it was noted that the Mach number had almost reached 1 at one point of the airfoil - 20 percent of the chord. It was thought that a jump to $M_1 = 0.8$ would be too great inasmuch as shock waves undoubtedly would appear before this time, so $M_1 = 0.75$ was the next solution attempted. After considerable effort, it was suspected that no solution could be obtained unless a shock wave were included, so this solution was temporarily dropped and $M_1 = 0.74$ was tried. This solution could not be obtained either so the Mach number was again dropped to $M_1 = 0.73$. For this case, a solution was obtained without serious trouble, and with this solution it was a relatively easy matter to return to the solution for $M_1 = 0.74$ and introduce a shock wave. The method by which it was found convenient to introduce the shock wave is instructive in that the numerical process here made use of some of the characteristics of a hyperbolic equation. The residuals that had not been removable in the first place in a solution for $M_1 = 0.74$ were distributed primarily in the supersonic region alongside of the airfoil. On returning to this solution, these residuals were moved back from column to column until all the residuals had been accumulated in two columns near the rear of the supersonic region. Then an attempt was made to introduce a shock wave, following the method described in the appendix of reference 6. If the two columns of residuals accurately

described a shock wave after a few attempts at adjustment, then a solution had been found. If not, the residuals were again moved downstream one column and the shock wave was again tried. After a few trials, it was found possible to get a solution with a shock wave present. The solutions for both $M_1 = 0.74$ and $M_1 = 0.75$ with the airfoil in the tunnel have shock waves. For the airfoil in free air, no shock waves were required at $M_1 = 0.75$. However, it was fairly certain that they would be required at $M_1 = 0.76$ or perhaps at a value of M_1 a trifle higher.

In figure 5 are shown the streamlines and constant Mach number lines for the airfoil in the wind tunnel at $M_1 = 0.75$. The shock wave touches the airfoil at 32 percent of the chord and bends upstream. Its total length is about 20 percent of the chord at this Mach number. For comparison, figure 6 shows the streamlines and constant Mach number lines for the airfoil in free air. No shock is present in this case, and the maximum Mach number on the airfoil is 1.10 rather than 1.165 for the airfoil in the tunnel. Before considering the details of these figures, it is well to look at the variation of Mach number along the airfoil as given in figures 7(a) and 7(b) and the pressure coefficient as given in figures 8(a) and 8(b). In these figures the pressure coefficient is defined by

$$C_p = \frac{p - p_1}{\frac{1}{2}\rho_1 q_1^2} = \frac{\frac{p}{p_0} - \frac{p_1}{p_0}}{\frac{1}{2}\frac{\rho_1 q_1^2}{p_0}} \tag{2}$$

This coefficient was computed from the stream-function values by using the computation curves presented in reference 5. The outstanding feature to be observed in figures 7(a) and 8(a) is the variation of Mach number and pressure coefficient when a shock wave is present, in particular the variation of these quantities immediately following the shock wave. The velocity and pressure coefficient, which have large magnitudes immediately preceding the shock, drop abruptly to values considerably below those appropriate to the corresponding quantities on the trailing portion of the airfoil. The pressure coefficient, in fact, even falls in magnitude below the corresponding incompressible-fluid coefficient. This extreme drop is immediately followed by a very rapid rise so that values on the trailing portion of the airfoil fall in about the position to be expected on extrapolation of values obtained at lower Mach numbers. This phenomenon, which in the present calculations verifies the findings described in reference 6 by actually having as many as three net points in the region of rise, is caused by the curvature condition described in reference 6. This appears so

important that a brief reiteration of the physical ideas seems worth while. Since the stream is required to follow the airfoil surface, the curvature of the streamlines adjacent to the surface is specified by that surface. Since the surface is everywhere convex, there must be a pressure increase normal to the airfoil surface in order to cause the velocity vector to turn as the fluid flows along the surface. Following the shock, however, the shock conditions have produced a pressure variation normal to the surface dependent on the pressure variation just prior to the shock, and in general for Mach numbers near 1 the pressure variation normal to the surface will be reversed by the shock. Hence the fluid must readjust itself very rapidly if it is to follow the airfoil surface. This curvature condition is responsible for the rapid pressure rise.

Some free-flight experimental pressure coefficients on an NACA 0012 airfoil at $\alpha = 0$ are given in figures 9 and 10. These data were obtained by The Glenn L. Martin Co. during the conduct of an investigation for the Navy Department. The experimental data were obtained by a wing-flow technique and are subject to a number of rather large experimental errors. The most important of these is the difficulty in maintaining a zero angle of attack. The pressure coefficients on the upper and lower surfaces were different and the average is plotted.

A comparison of figures 8(b) and 9 shows many common general features. The pressure coefficient falls (in magnitude) with increase of Mach number near the nose; elsewhere the reverse is true. The pressure peak moves up at first slowly, then more rapidly with increase of Mach number. At the same time, the pressure peak moves away from the nose.

If, at the point along the airfoil where the experimental data are unsteady, a normal shock wave is assumed, the dashed sections of the graph of figure 9 are obtained. These agree qualitatively very well with the computed results of figure 8(a). With boundary layer the shock wave will usually be oblique.

In figure 5 some details of the process of adjustment are indicated by the occurrence of a saddle point in the Mach number surface, which to the accuracy of the present solutions appears to be at $M_1 = 0.915$. Another interesting, though less spectacular, result may be noted. The maximum Mach number on the airfoil surface increases more and more rapidly as the undisturbed-stream Mach number increases and the point on the chord on which the maximum Mach number occurs moves toward the trailing edge. At the higher undisturbed-stream Mach numbers, the pressure coefficient near the leading edge tends to fall below those for lower Mach numbers. It should also be observed that the shock wave does not occur on the airfoil surface at the point where the highest Mach number exists. For example, for $M_1 = 0.75$ the maximum Mach number M_{max} on the airfoil surface occurs at 26 percent of the chord

and is 1.165. The Mach number then falls to $M = 1.140$ immediately before the shock wave, which is at 32 percent of the chord. After the shock wave, the Mach number is 0.875 and rises rapidly to a maximum of $M = 0.955$ before falling in the customary way along the rear half of the airfoil.

A comparison of the variation of pressure coefficient along the chord as affected by the wind-tunnel walls is shown in figure 11 for an undisturbed-stream Mach number M_1 equal to 0.70. This figure should be compared with figure 3, where the corresponding incompressible coefficients are plotted. For $M_1 = 0.70$ the difference in pressure coefficient is about 18 percent of the maximum, a considerably larger difference than the 4 percent of the incompressible case. The curves, however, are still quite smooth, and it would be expected, therefore, that a reasonably simple approximate theory might serve to predict this difference. The difference between the pressure coefficient for a compressible flow with a shock wave and the incompressible fluid flow varies considerably from one point to another along the airfoil and at maximum is almost equal to one-third of the maximum coefficient. (See fig. 12.)

Comparison has been made between the relaxation solution for the effect of compressibility and the predictions made on the basis of a number of current approximate theories. In figures 13 and 14, two cases are plotted - the first for $M_1 = 0.73$ and the second for $M_1 = 0.60$. The approximate theories noted for comparison are given by the following equations: From Prandtl and Glauert (references 1 and 2, respectively),

$$C_{p_M} = \frac{C_{p_0}}{\left(1 - M_1^2\right)^{1/2}} \tag{3}$$

from Von Kármán and Tsien (references 3 and 4, respectively),

$$C_{p_M} = C_{p_0} \frac{1}{\left(1 - M_1^2\right)^{1/2} + \dfrac{M_1^2}{1 + \left(1 - M_1^2\right)^{1/2}} \dfrac{C_{p_0}}{2}} \tag{4}$$

and from the assumption of proportionality of kinetic energy,

$$q_i^2 = \left(\frac{q^2}{q_1^2}\right)_0 = \left(\frac{\frac{1}{2}\frac{\rho q^2}{p_0}}{\frac{1}{2}\frac{\rho_1 q_1^2}{p_0}}\right)_M \tag{5}$$

Values of $\frac{1}{2}\frac{\rho q^2}{p_0}$ were obtained from computation curve 13, figure 24 of reference 5. From Temple-Yarwood (reference 12),

$$q_i = \frac{\left(1 + \frac{\gamma - 1}{2}M_1^2\right)^2}{\left(1 + \frac{\gamma - 1}{2}M^2\right)^2} \frac{M^2}{M_1^2} \frac{1 - \frac{\gamma - 1}{8}M^2}{1 - \frac{\gamma - 1}{8}M_1^2} \tag{6}$$

and from Garrick-Kaplan (reference 13),

$$q_i = \left(\frac{\tau}{\tau_1}\right)_M \frac{e^{\frac{1}{2}\left[f(\tau)+g(\tau)\right]}}{e^{\frac{1}{2}\left[f(\tau_1)+g(\tau_1)\right]}}$$

where

$$\left.\begin{aligned} \tau &= \frac{M^2}{\frac{2}{\gamma - 1} + M^2} \\ f(\tau) &= \frac{1}{2}\int_0^{\tau} (1 - \tau)^{\frac{1}{\gamma - 1}} \frac{d\tau}{\tau} \\ g(\tau) &= \frac{1}{2}\int_0^{\tau} \left[\frac{1 - \frac{\gamma + 1}{\gamma - 1}\tau}{(1 - \tau)^{\frac{\gamma}{\gamma - 1}}} - 1\right]\frac{d\tau}{\tau} \end{aligned}\right\} \tag{7}$$

It is to be noted that all these theories are within ±10 percent of the relaxation solution and the Von Kármán-Tsien equation gives almost exactly the same result as the relaxation solution up to $M_1 = 0.6$. However, it is to be noted that all the theories deviate very badly at $M_1 = 0.73$, which, it should remembered, is very close to the first appearance of shock waves. Cross plots of the pressure coefficient for 20 and 30 percent of the chord are shown as figures 15 and 16, respectively. Here again it is obvious that the approximate theories are good until about $M_1 = 0.6$ after which the deviations become considerable. Following the appearance of shock waves, the approximate theories become completely worthless.

It might be well at this point to tabulate a few special values obtained from the solutions which should be checked against experimental results when these are available.

Test condition	Mach number on the airfoil surface first reaches 1 at -		The first shock wave appears at -	
	Percent of chord	M_1	Percent of chord	M_1
Airfoil in tunnel	20.5	0.710	25	0.73+
Airfoil in free air	17.2	.725	[a]22	[a].75+

[a]Free-air solution with shock not carried out. These approximate values obtained by extrapolation.

CONCLUSIONS

Calculation by the relaxation method of the effects of compressibility on the flow about the NACA 0012 airfoil at zero angle of attack in a wind tunnel and in free air yields the following general conclusions:

1. Pressure-coefficient and Mach number variations along the NACA 0012 airfoil in a wind tunnel and in free air were greater than experimental results because the boundary layer was neglected in the computations.

2. Comparisons of the relaxation solutions with the predictions of several approximate theories showed most of the latter to fall considerably too low at high Mach numbers. The present theory is in better agreement with experimental results on this airfoil.

3. Because of the requirement of continuity of streamline curvature across the shock at the surface of the airfoil, the discontinuous drop of pressure-coefficient magnitude through the shock is followed by a rapid rise. This rapid rise accounts for the experimental fact that the fall in magnitude of pressure coefficient as measured is never as large as that to be expected from the measured Mach number before the shock.

4. Although the relaxation method appears to be adequate to solve the very involved differential equations and boundary conditions describing the flow of a compressible fluid, the calculations are too involved to permit the investigation of a very wide range of interesting cases without the use of high-speed calculating machines.

5. A number of important experimentally observed effects, especially in the post-critical transonic zone, are not adequately described by the present theory of frictionless adiabatic perfect gas plus shock-wave discontinuities when necessary. No analytical solutions with this model fluid can be more adequate than the present results. To describe experimental results better requires the inclusion of the boundary layer.

Harvard University
Cambridge, Mass., May 7, 1946

REFERENCES

1. Prandtl, L.: Über Stromungen, derer Geschwindigkeit mit der Schallgeschwindigkeit vergleichbar sind. Jour. Aero. Res. Inst. Univ. Tokio, no. 6, 1930, p. 14.

2. Glauert, H.: The Effect of Compressibility on the Lift of an Aerofoil. R. & M. No. 1135, British A.R.C., 1927.

3. Von Kármán, Th.: Compressibility Effects in Aerodynamics. Jour. Aero. Sci., vol. 8, no. 9, July 1941, pp. 337-356.

4. Tsien, Hsue-Shen: Two-Dimensional Subsonic Flow of Compressible Fluids. Jour. Aero. Sci., vol. 6, no. 10, Aug. 1939, pp. 399-407.

5. Emmons, Howard W.: The Numerical Solution of Compressible Fluid Flow Problems. NACA TN No. 932, 1944.

6. Emmons, Howard W.: The Theoretical Flow of a Frictionless, Adiabatic, Perfect Gas inside of a Two-Dimensional Hyperbolic Nozzle. NACA TN No. 1003, 1946.

7. Green, J. R., and Southwell, R. V.: Relaxation Methods Applied to Engineering Problems. IX - High Speed Flow of Compressible Fluid through a Two-Dimensional Nozzle. Proc. Roy. Soc., ser. A, no. 808, vol. 239, April 1944, pp. 367-386.

8. Fox, L., and Southwell, R. V.: On the Flow of Gas through a Nozzle with Velocities Exceeding the Speed of Sound. Proc. Roy. Soc., ser. A, vol. 183, Aug. 1944, pp. 38-54.

9. Theodorsen, T., and Garrick, I. E.: General Potential Theory of Arbitrary Wing Sections. NACA Rep. No. 452, 1933.

10. Garrick, I. E.: Determination of the Theoretical Pressure Distribution for Twenty Airfoils. NACA Rep. No. 465, 1933.

11. Thom, A.: Blockage Corrections and Choking in a Closed High-Speed Tunnel. R. & M. No. 2033, British A.R.C., Nov. 1943.

12. Temple, G., and Yarwood, B.: The Approximate Solution of the Hodograph Equations for Compressible Flow. Rep. No. S.M.E. 3201, British R.A.E., June 1942.

13. Garrick, I. E., and Kaplan, Carl: On the Flow of a Compressible Fluid by the Hodograph Method. I - Unification and Extension of Present-Day Results. NACA Rep. No. 789, 1944.

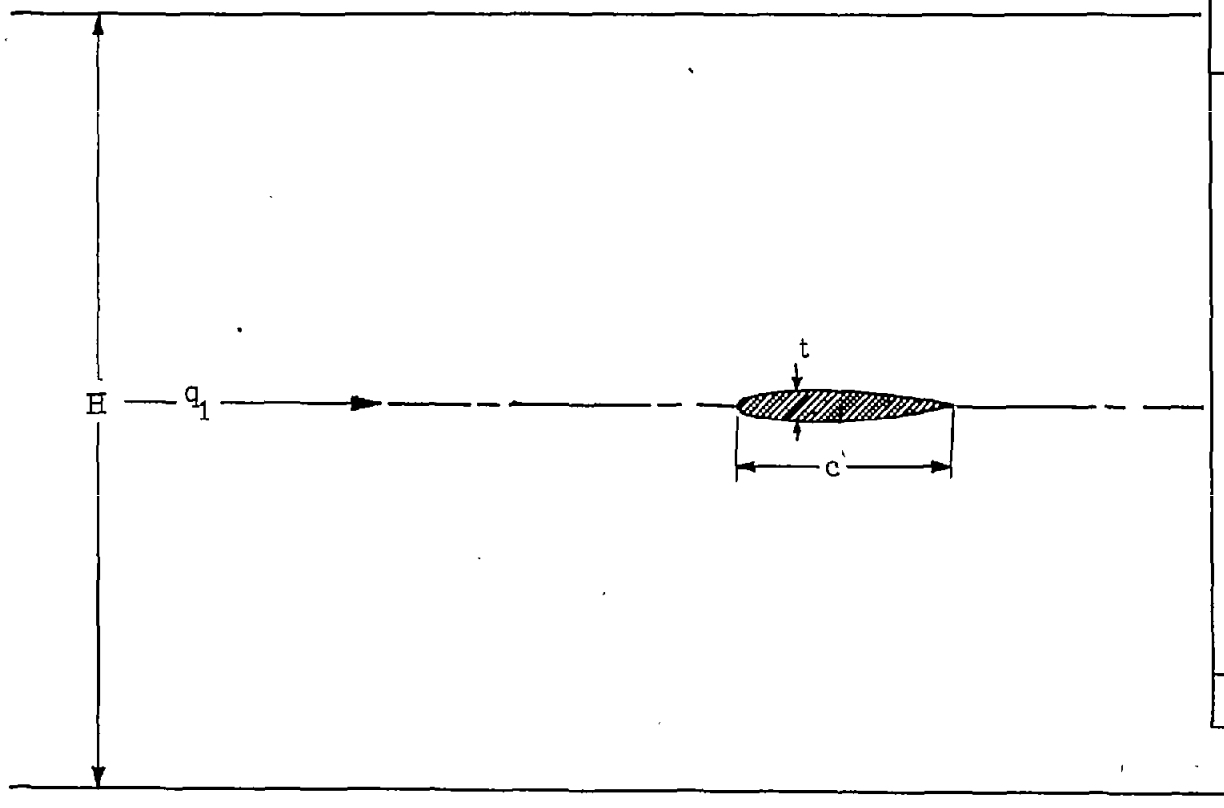

Station (percent c)	Ordinate (percent c)
0	0
1.25	1.894
2.5	2.615
5.0	3.555
7.5	4.200
10	4.683
15	5.345
20	5.738
25	5.941
30	6.002
40	5.803
50	5.294
60	4.563
70	3.664
80	2.623
90	1.448
95	.807
100	0
L.E. radius: 1.58 percent c	

Figure 1.- The problem calculated. NACA 0012 airfoil at zero angle of attack on center line of a wind tunnel and in free air, that is, with tunnel walls removed. $\frac{t}{c} = 0.12$; $\frac{H}{c} = 3.6$; $\frac{H}{t} = 30$.

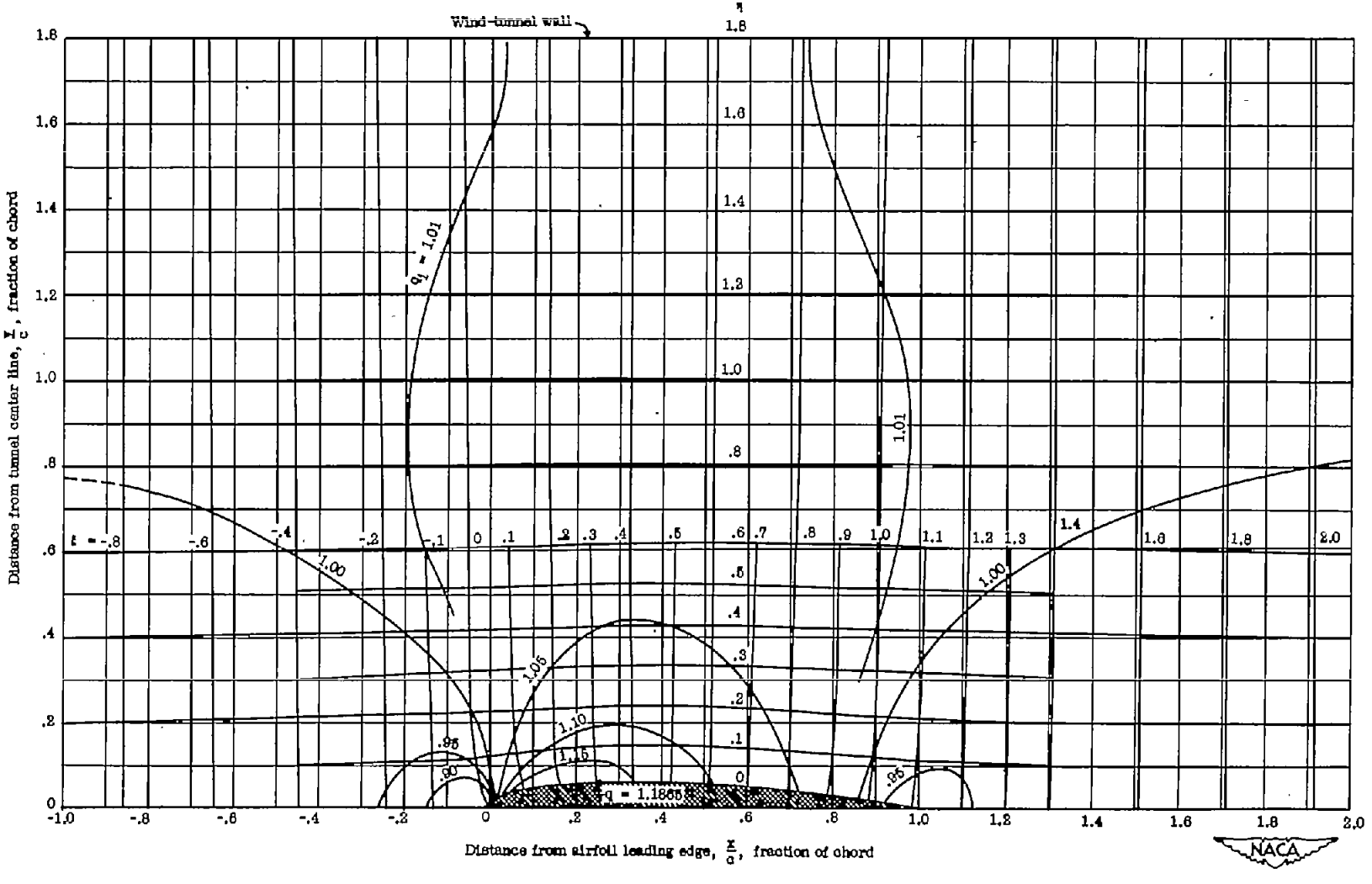

Figure 2.- Streamlines and equipotential lines for the flow of an incompressible fluid past an NACA 0012 airfoil in a wind tunnel. $\alpha = 0$; $M_1 = 0$. Constant velocity lines shown for various values of q_1.

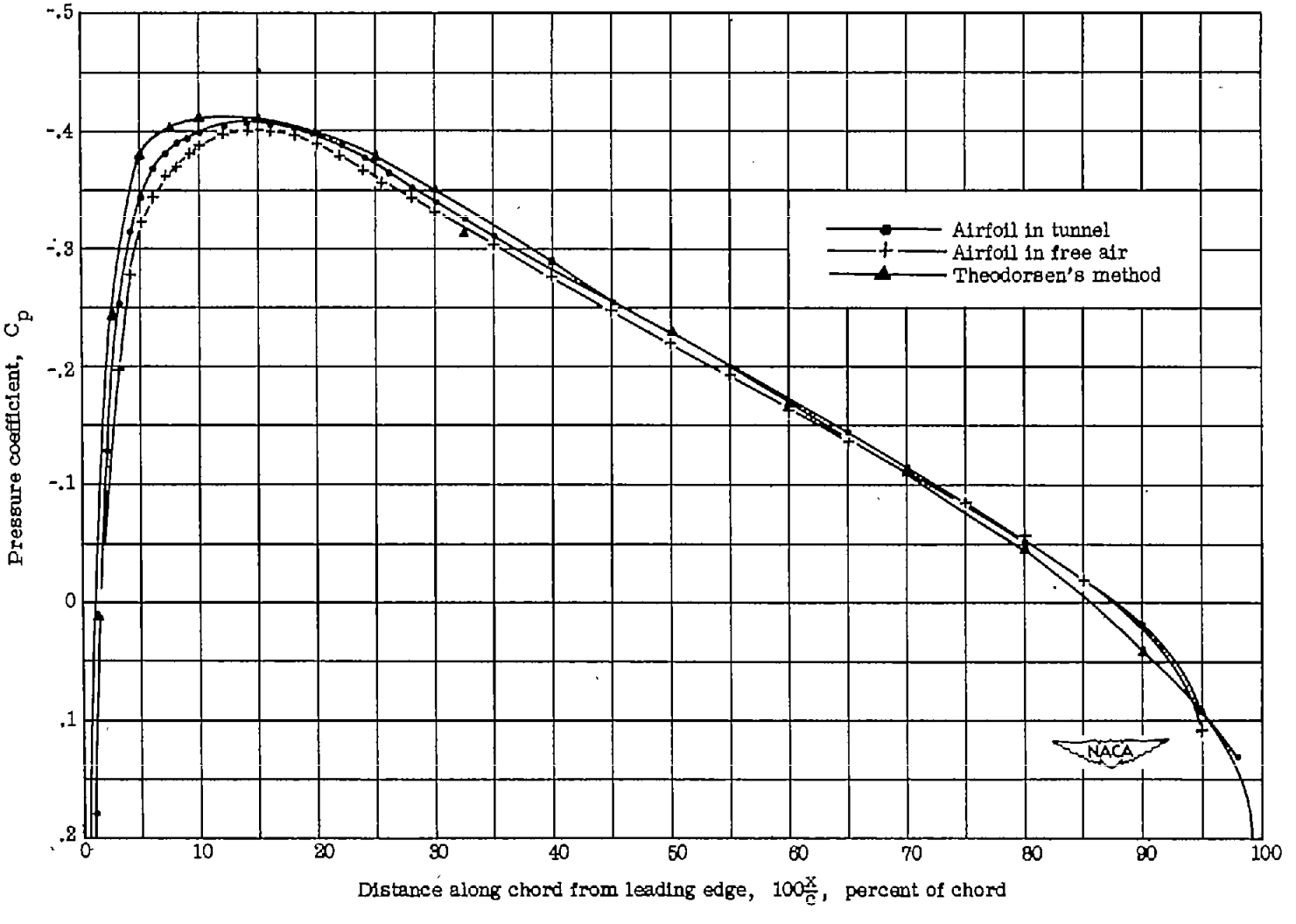

Figure 3.- Effect of wind-tunnel walls on pressure-coefficient variation along chord of NACA 0012 airfoil. $\alpha = 0$; $M = 0$.

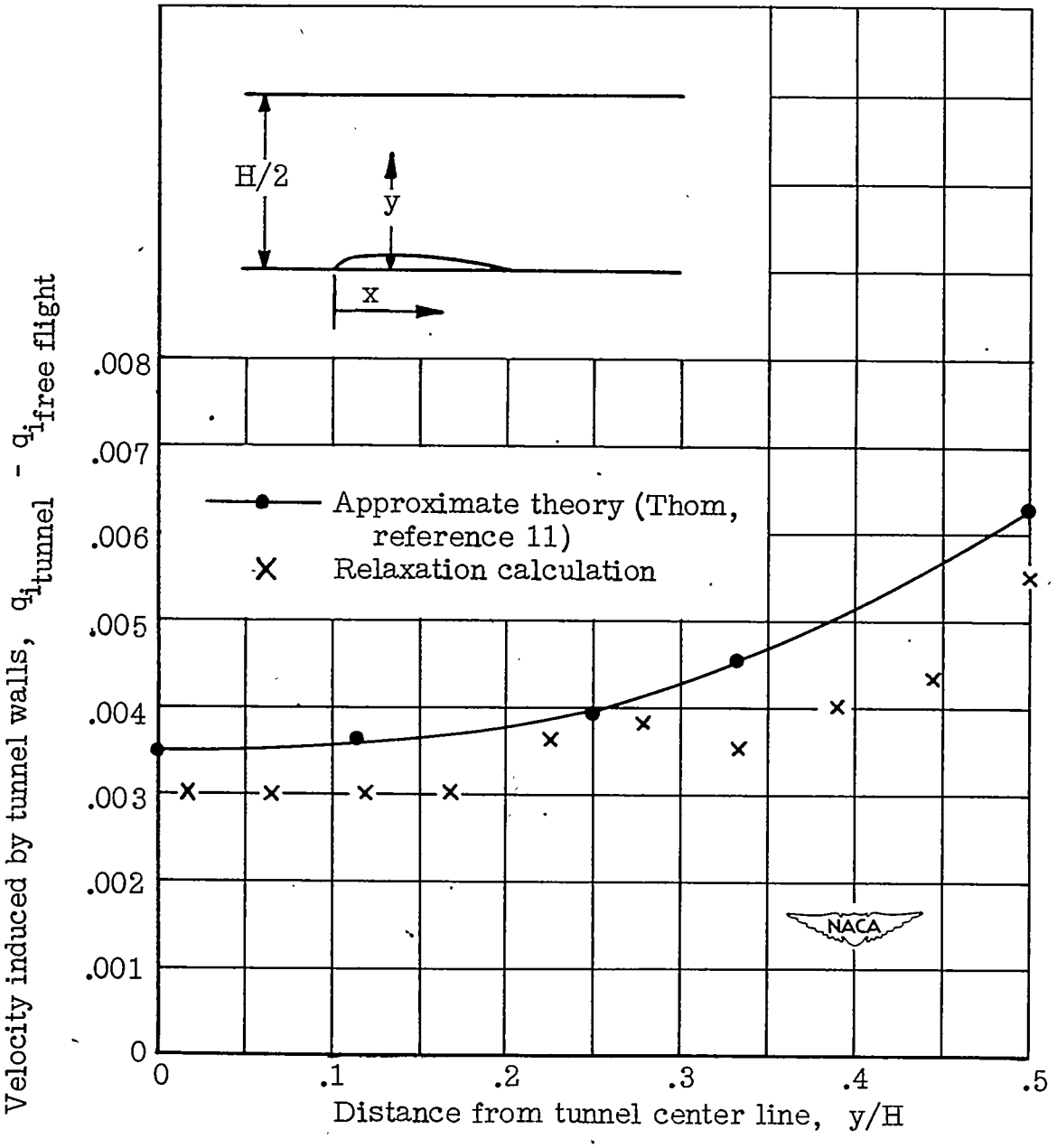

Figure 4.- Velocity induced by wind-tunnel walls in narrowest section between airfoil and tunnel.

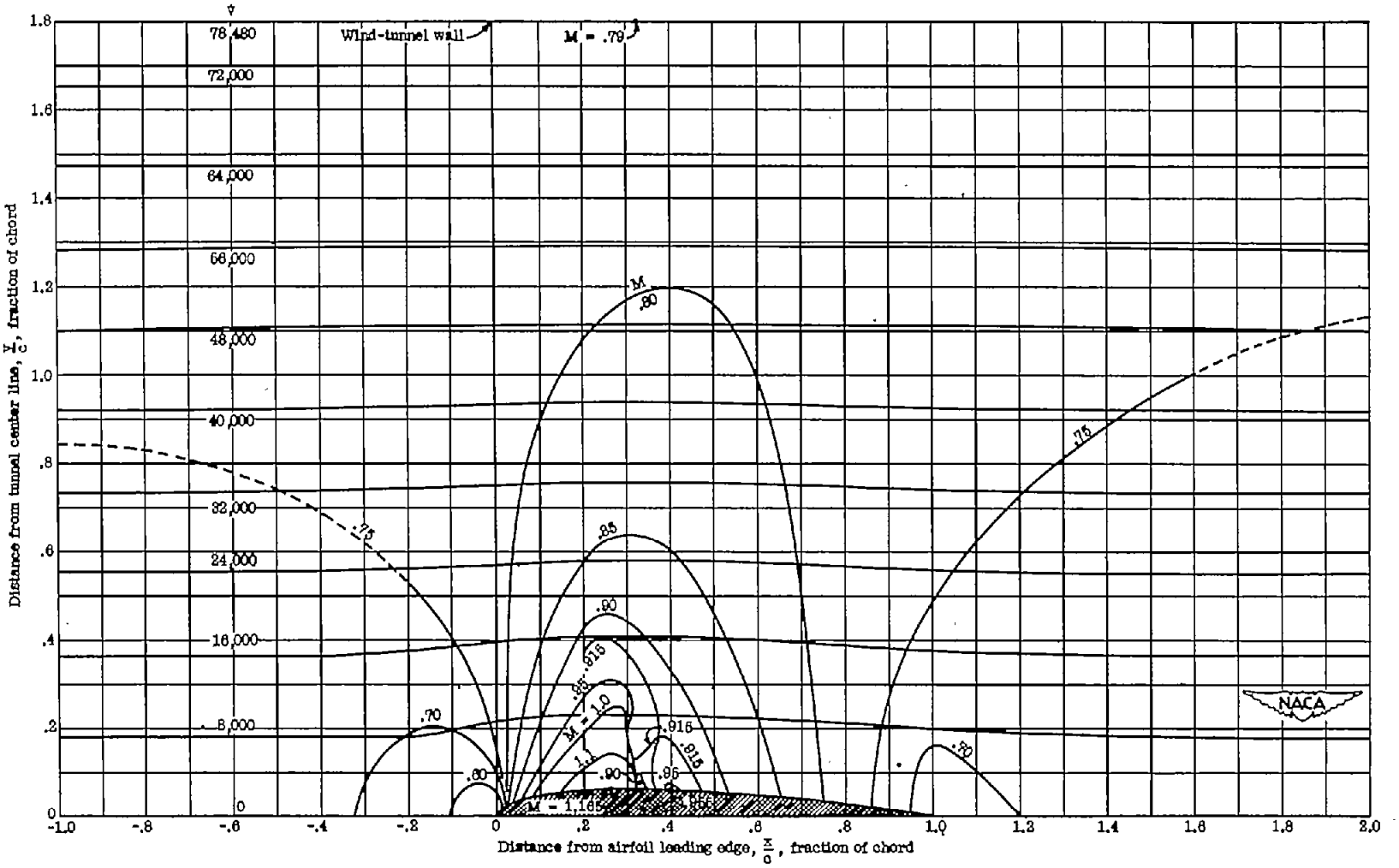

Figure 5.- Streamlines and constant Mach number lines for flow of a compressible fluid past an NACA 0012 airfoil in a wind tunnel. $\alpha = 0$; $M_1 = 0.75$.

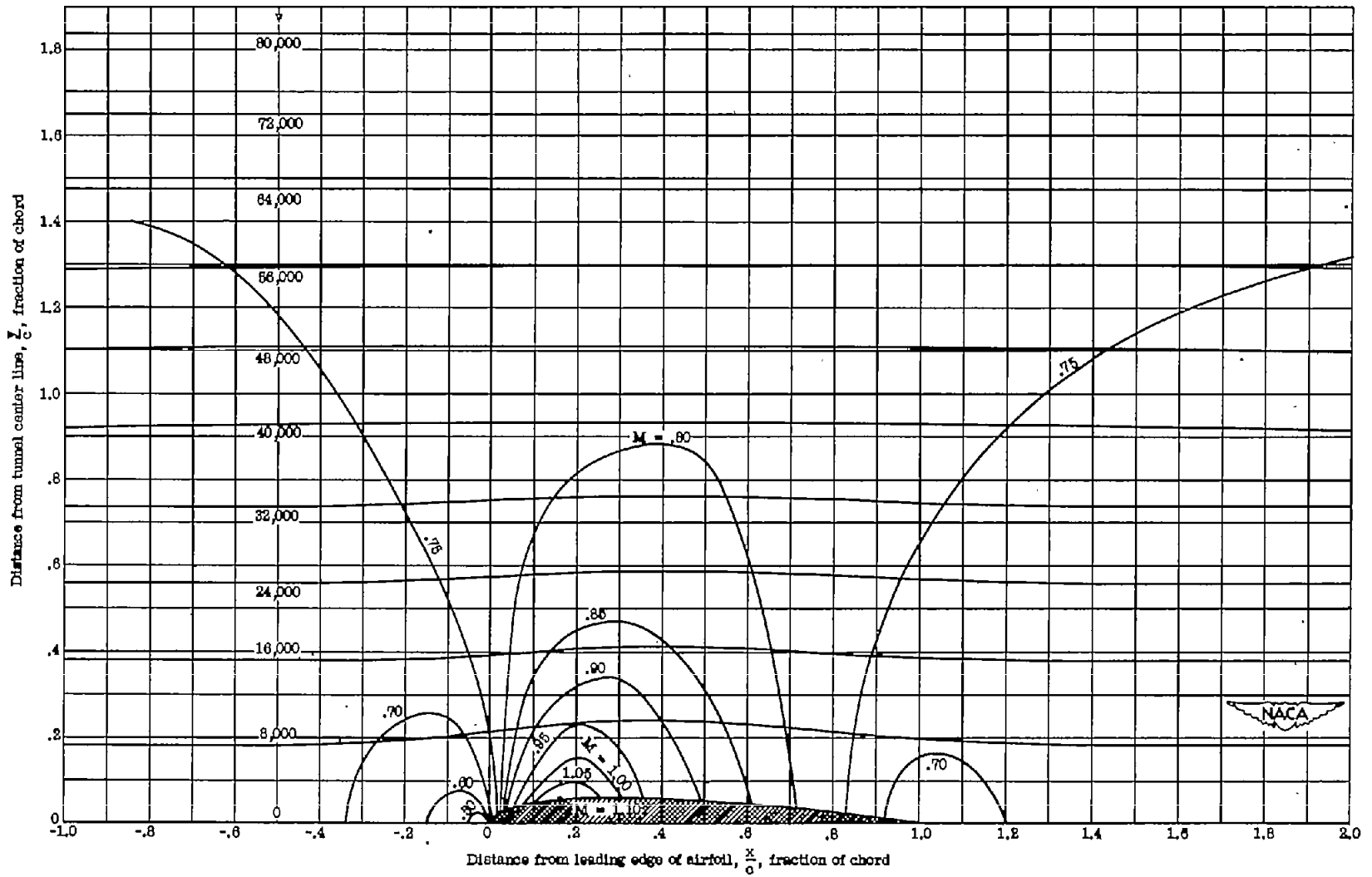

Figure 6.- Streamlines and constant Mach number lines for flow of a compressible fluid past an NACA 0012 airfoil in free air. $\alpha = 0$; $M_1 = 0.75$.

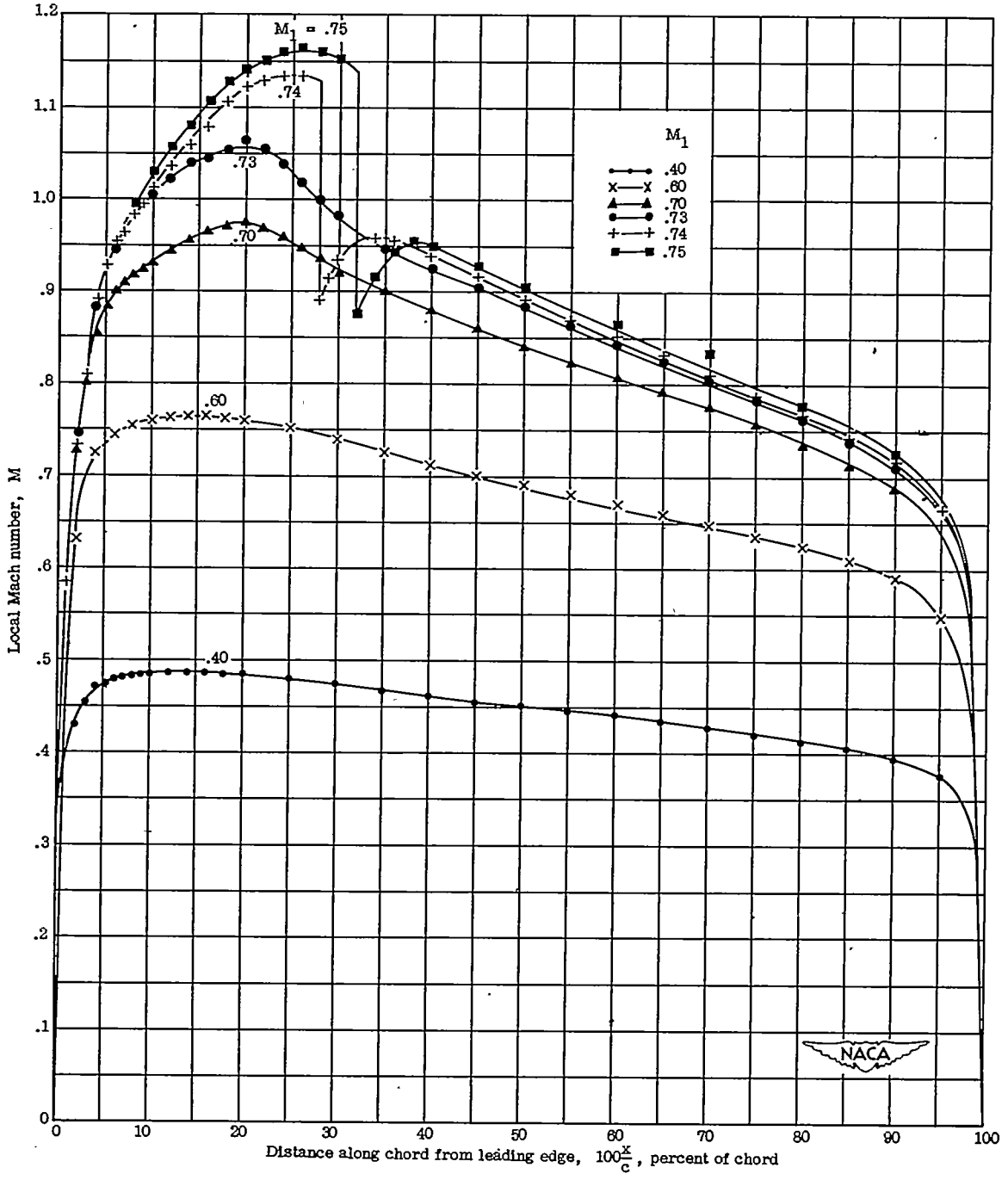

(a) In wind tunnel.

Figure 7.- Mach number distribution for NACA airfoil. $\alpha = 0$.

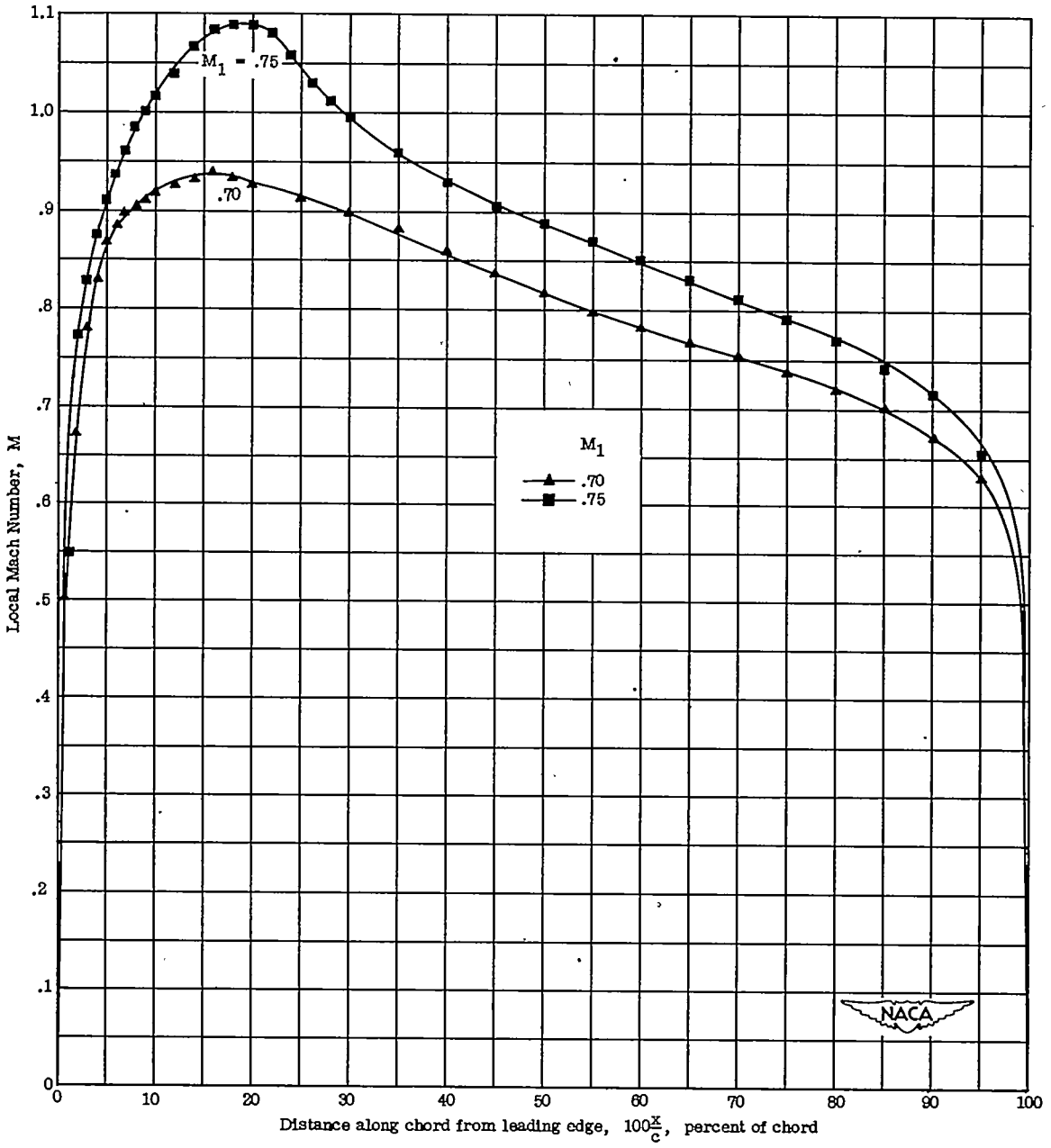

(b) In free air.

Figure 7.- Concluded.

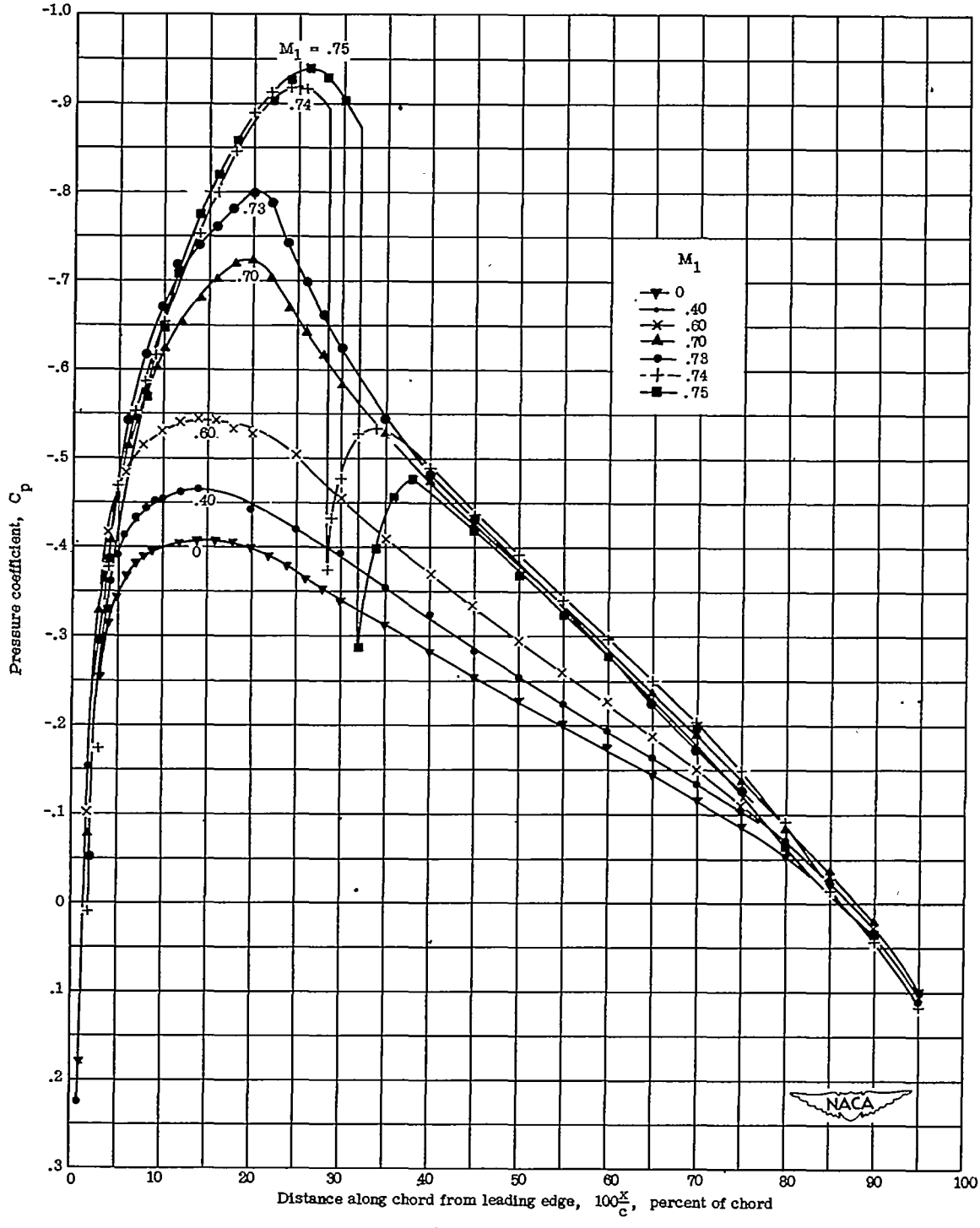

(a) In wind tunnel.

Figure 8.- Calculated pressure distribution for NACA 0012 airfoil. $\alpha = 0$.

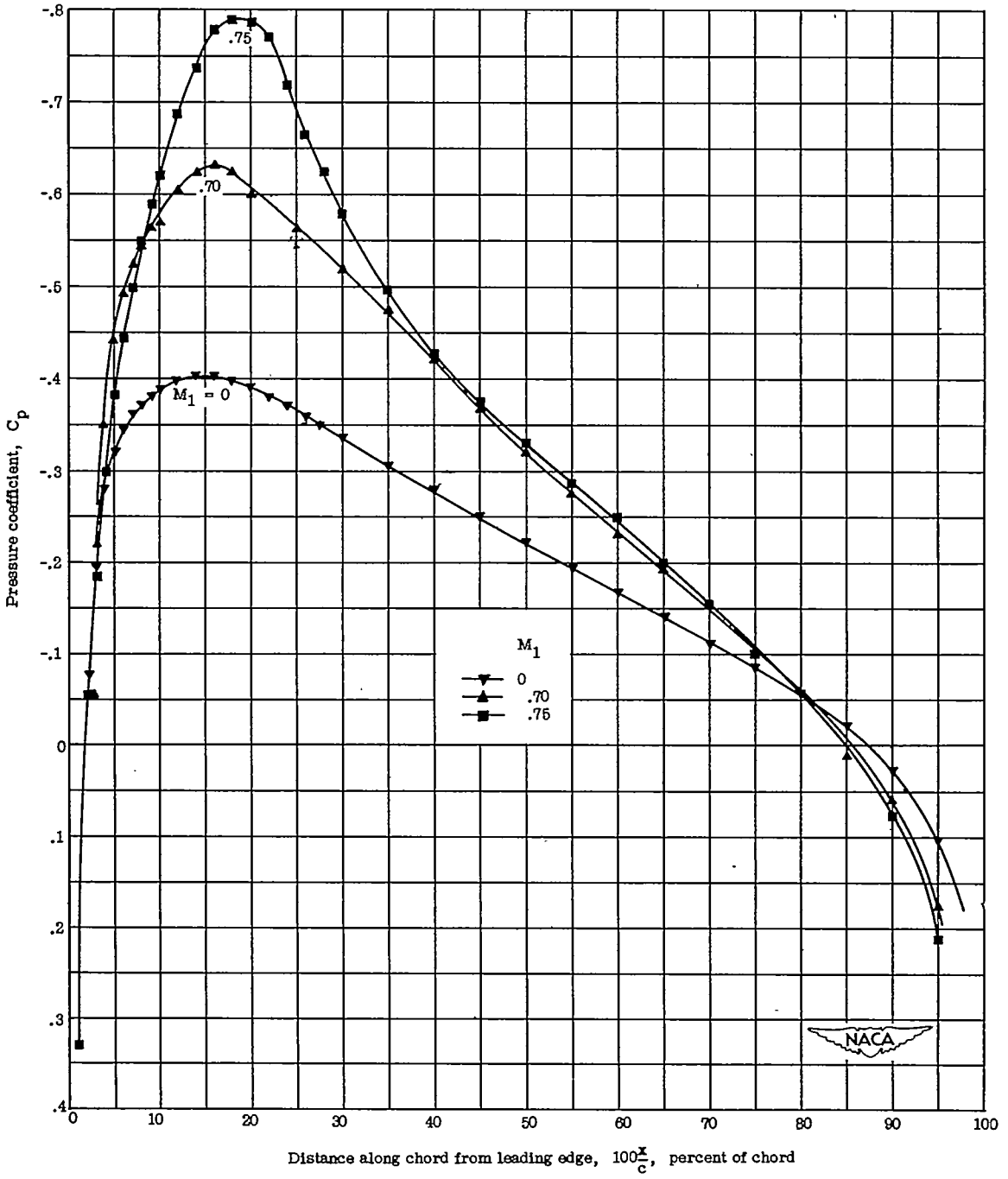

(b) In free air.

Figure 8.- Concluded.

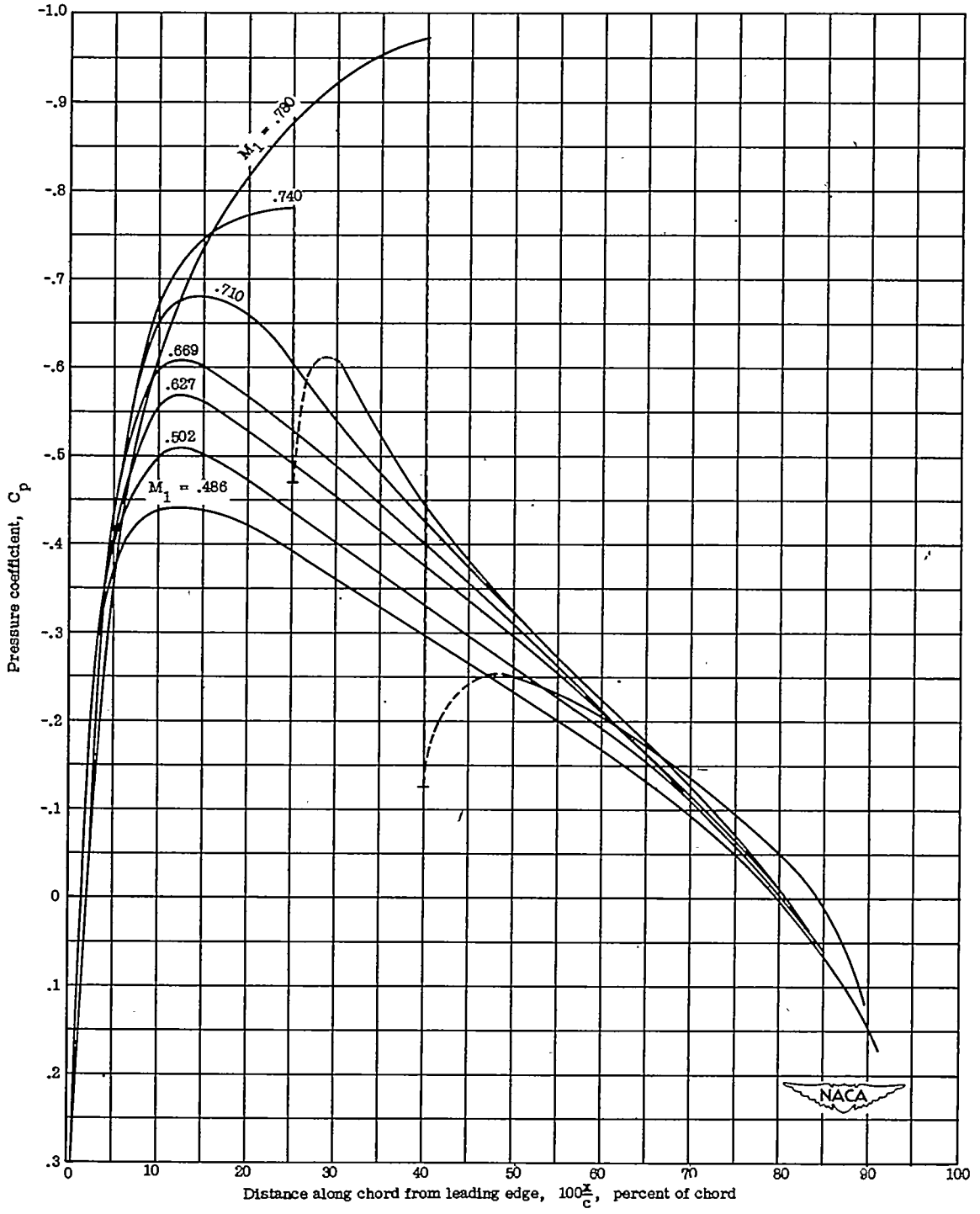

Figure 9.- Experimental free-flight pressure distribution for the NACA 0012 airfoil. $\alpha \approx 0$. Since α was not precisely zero, the values plotted represent an average of the measured pressures on the upper and lower surfaces.

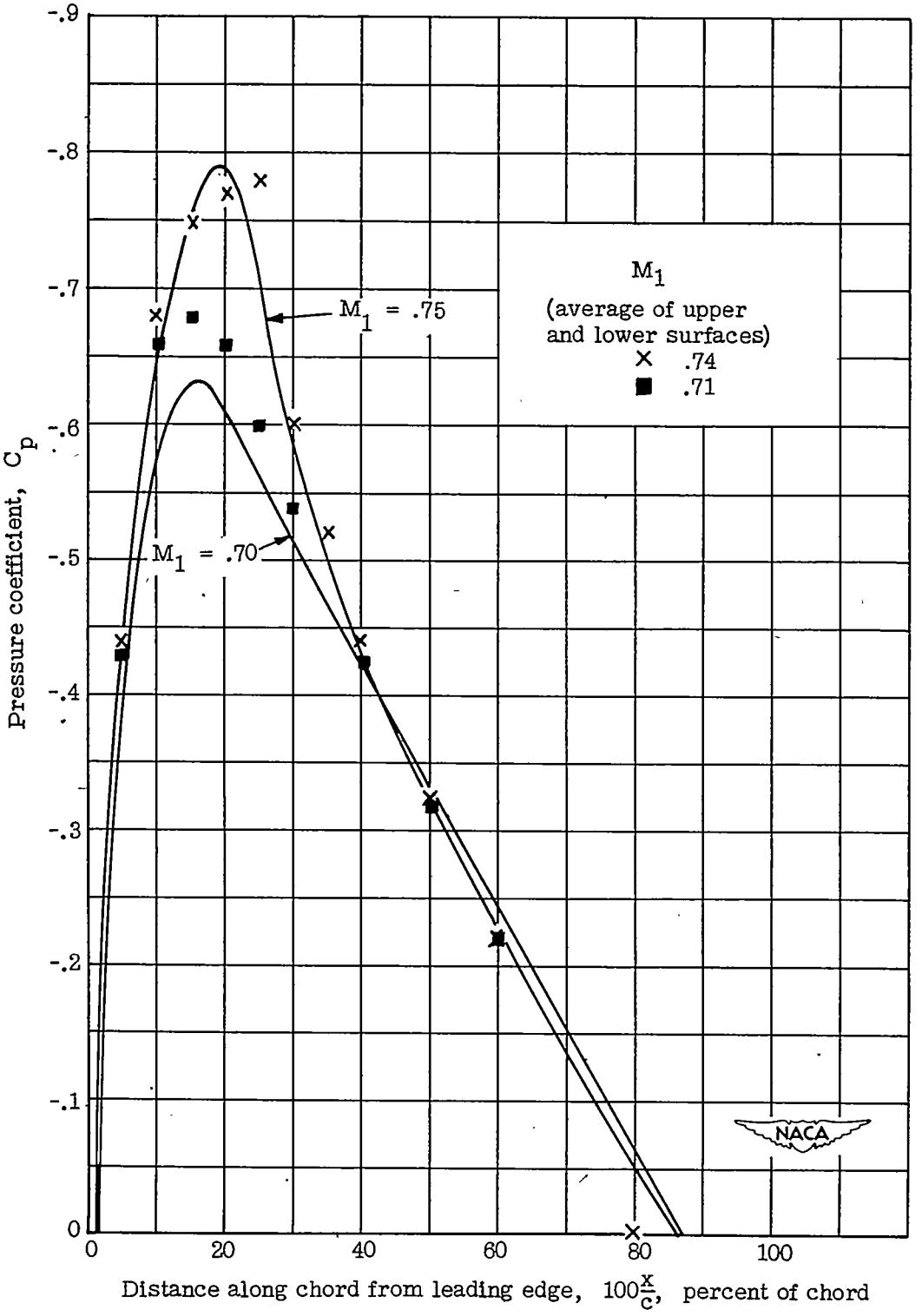

Figure 10.- Comparison of relaxation solution with experimental pressure distribution for NACA 0012 airfoil at $\alpha = 0$ from flight tests. Curves indicate calculated results. Points indicate experimental results.

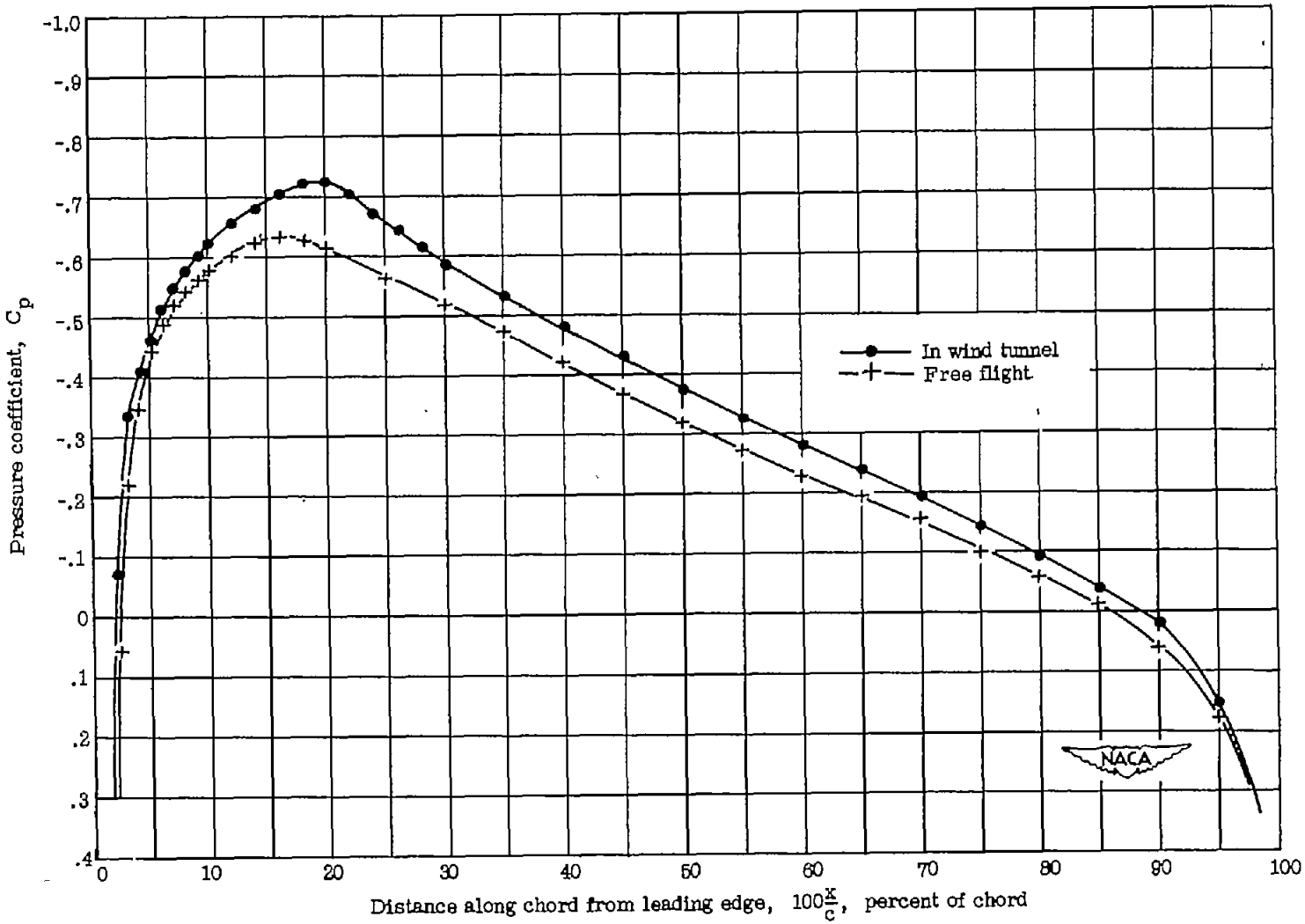

Figure 11.- Comparison of pressure distributions for NACA 0012 airfoil in wind tunnel and in free air. $\alpha = 0$; $M_1 = 0.70$.

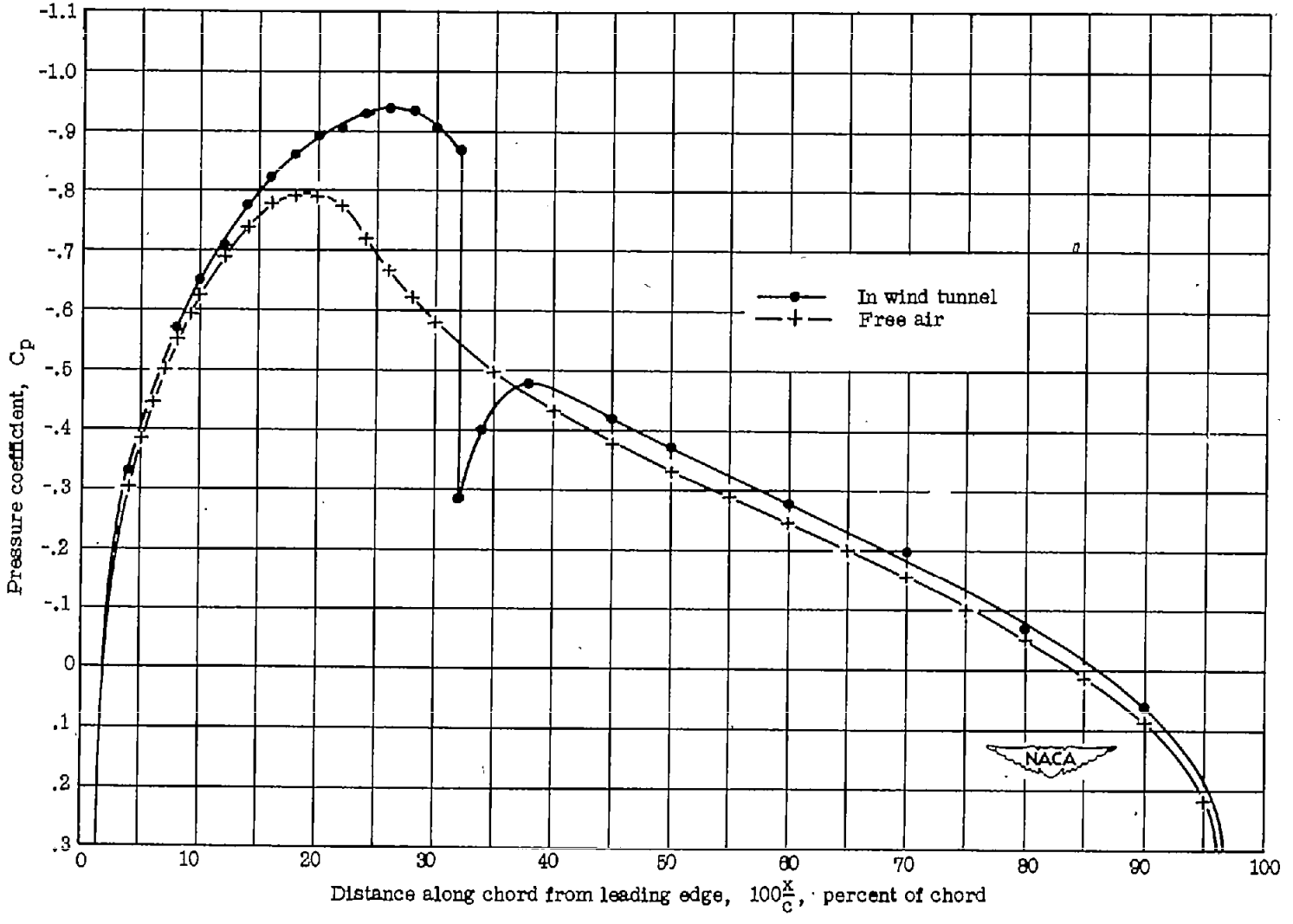

Figure 12.- Comparison of pressure distributions for NACA 0012 airfoil in wind tunnel and in free air. $\alpha = 0$; $M_1 = 0.75$.

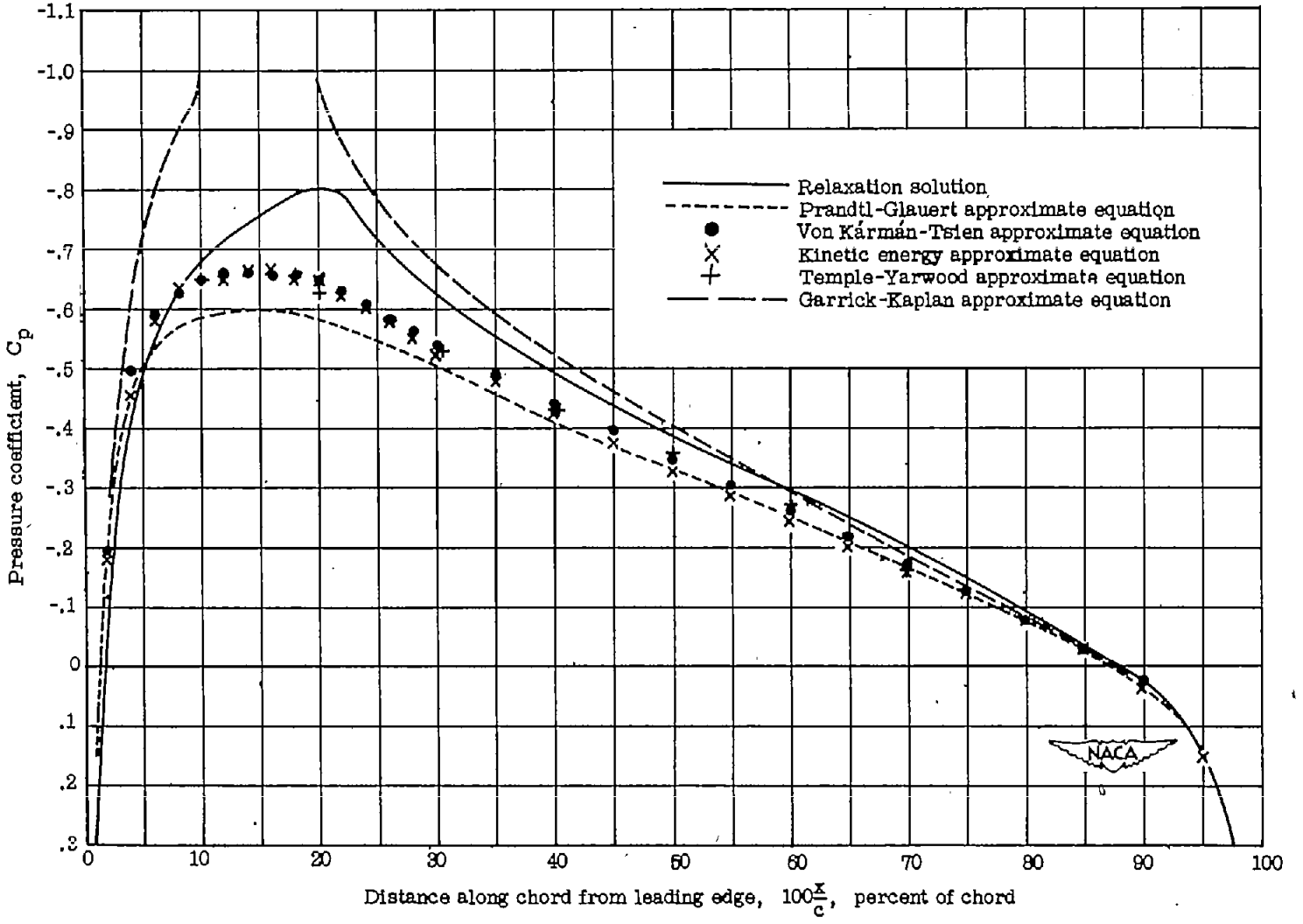

Figure 13.- Comparison of relaxation solution with approximate formulas for pressure distributions for NACA 0012 airfoil in a wind tunnel. $\alpha = 0$; $M_1 = 0.73$. The compressibility correction equations were applied to the incompressible relaxation solution for the NACA 0012 airfoil in a wind tunnel. (Corrections applied to curve $M_1 = 0$ (fig. 8a).)

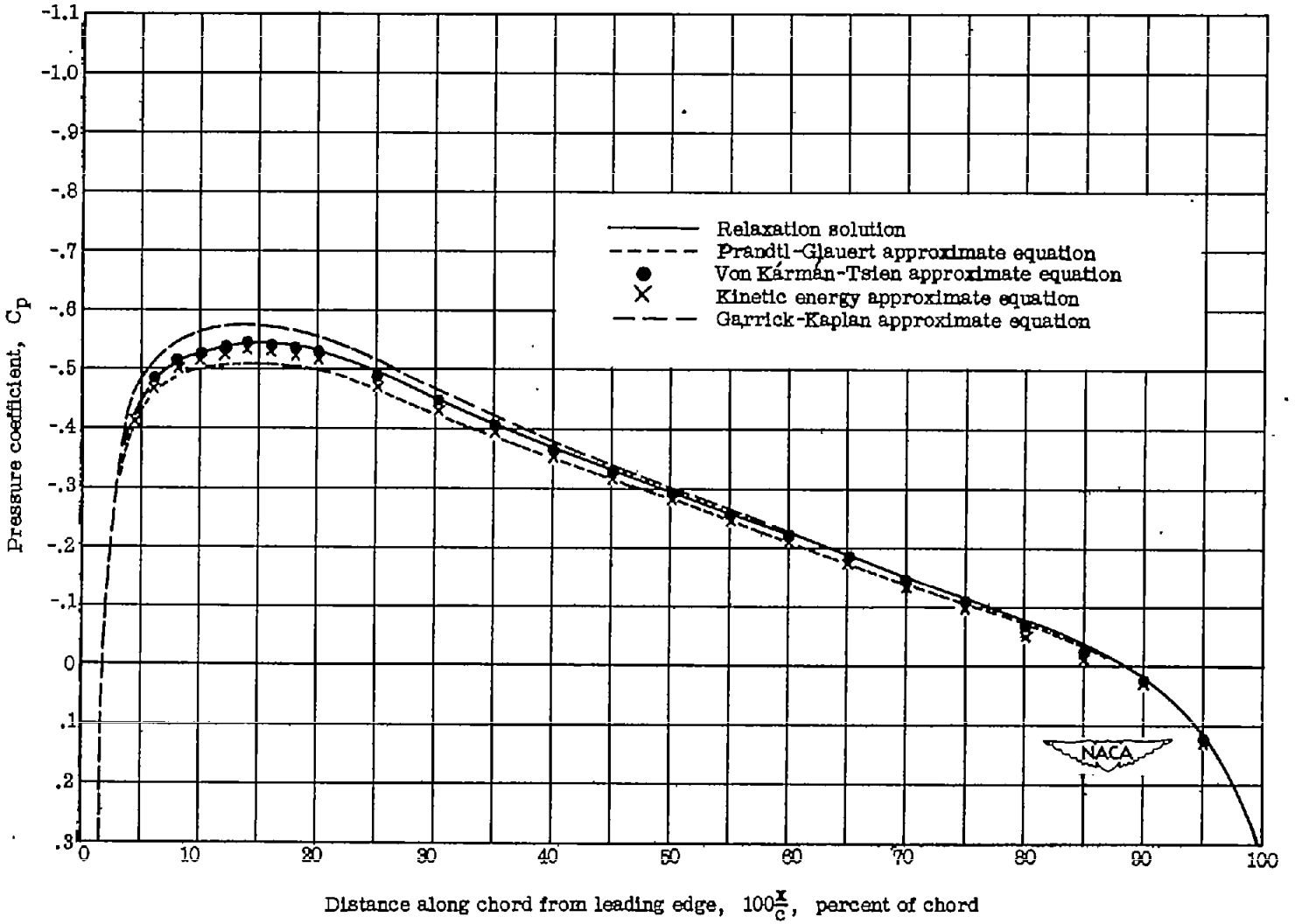

Figure 14.- Comparison of relaxation solution with approximate formulas for pressure distributions for NACA 0012 airfoil in a wind tunnel. $\alpha = 0$; $M_1 = 0.60$. (Corrections applied to curve $M_1 = 0$ (fig. 8a).)

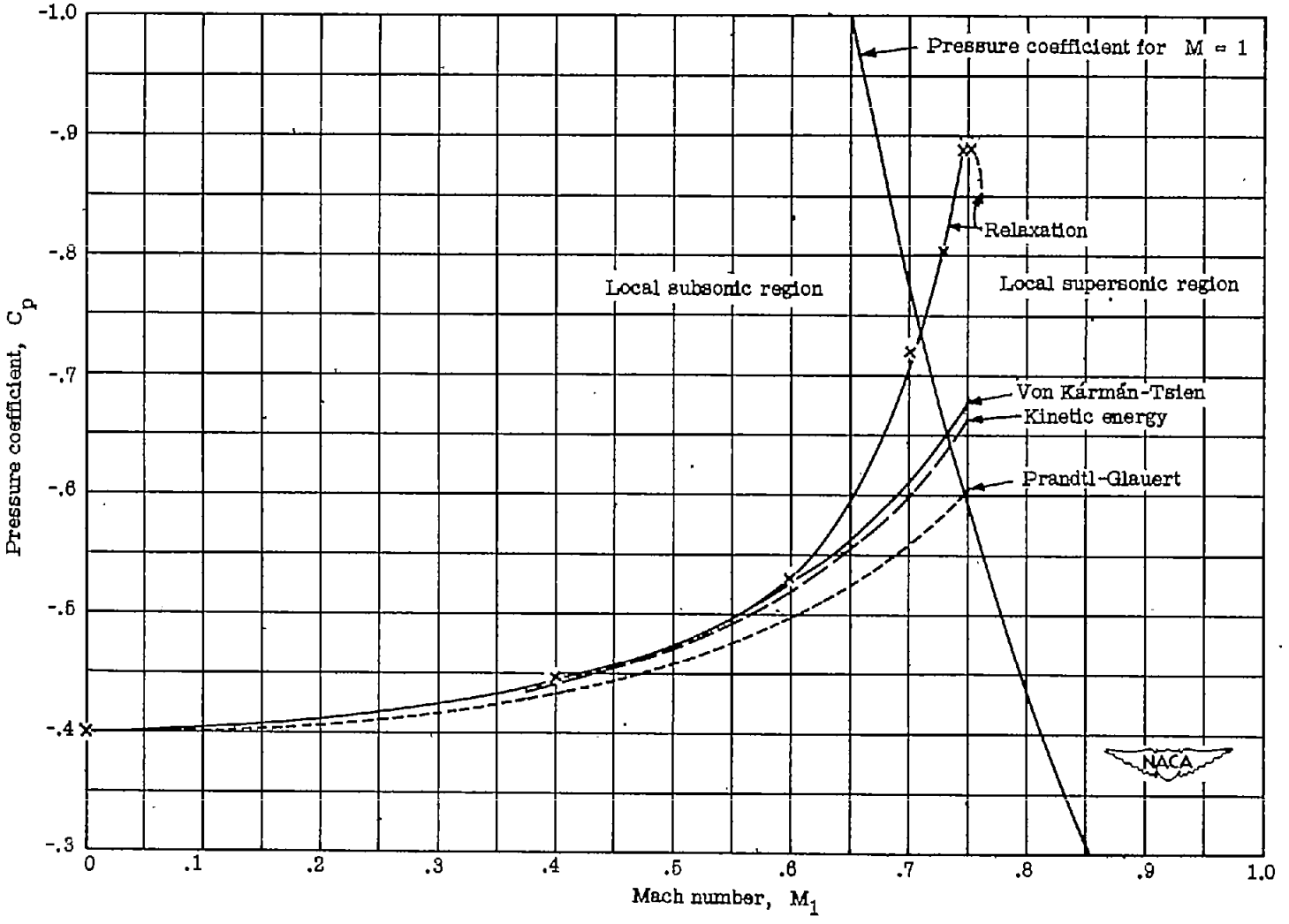

Figure 15.- Comparison of relaxation solution with approximate formulas for variation of pressure coefficient with Mach number at 20 percent of chord for NACA 0012 airfoil in a wind tunnel.

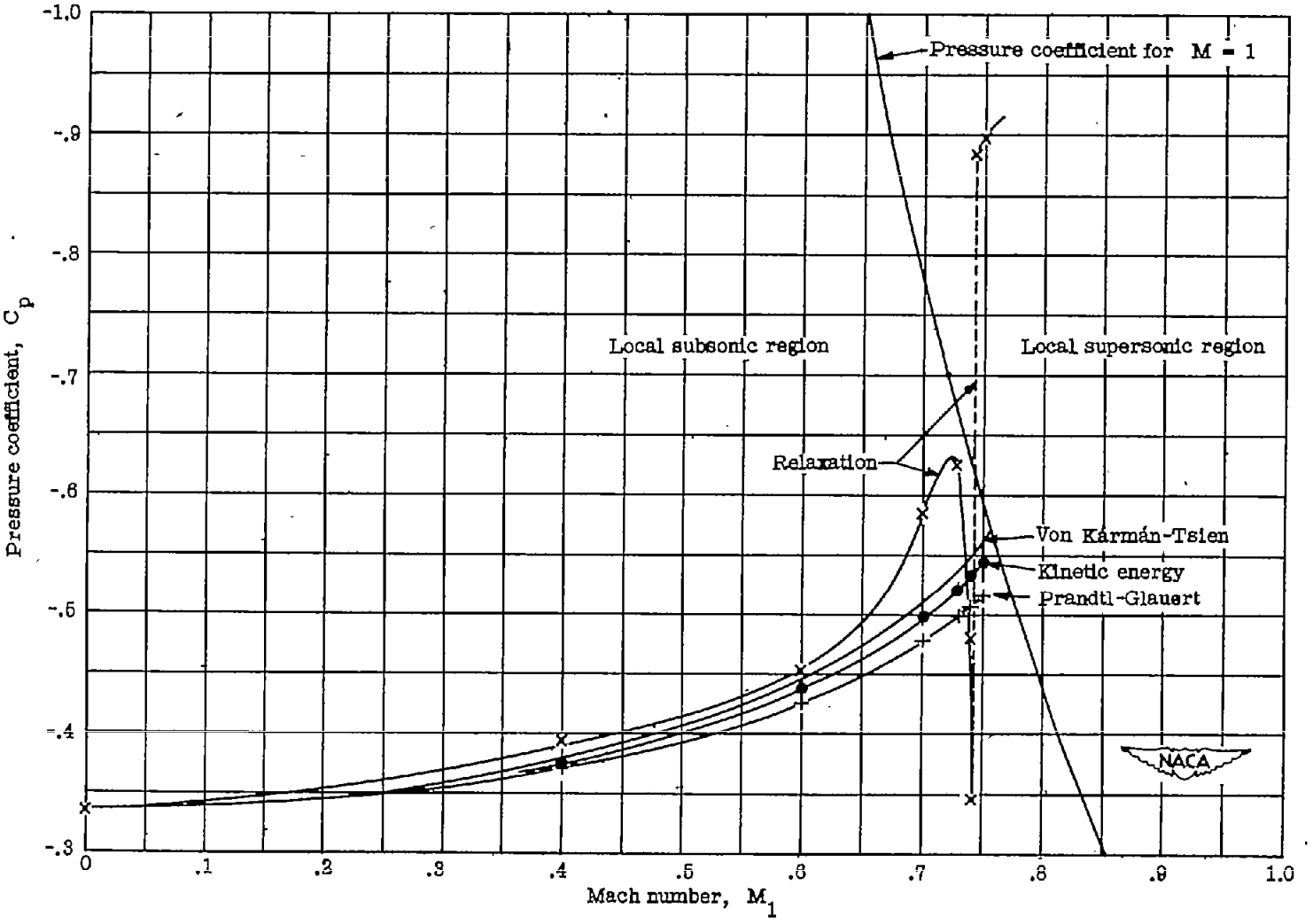

Figure 16.- Comparison of relaxation solution with approximate formulas for variation of pressure coefficient with Mach number at 30 percent of chord for NACA 0012 airfoil in a wind tunnel.